Catalysis Today 216 (2013) 240–245

Contents lists available at SciVerse ScienceDirect

Catalysis Today

journal homepage: www.elsevier.com/locate/cattod

Fe–B catalyst fabricated by hybrid capacitive adsorption–chemical reduction method and its application for hydrogen production from $NaBH_4$ solution

Trinh Ngoc Tuan [a], Youngmi Yi [a], Jae Kwang Lee [b], Jaeyoung Lee [a,b,*]

[a] Electrochemical Reaction and Technology Laboratory (ERTL), School of Environmental Science and Technology, Gwangju 500-712, South Korea
[b] Ertl Center for Electrochemistry and Catalysis, RISE, Gwangju Institute of Science and Technology, Gwangju 500-712, South Korea

ARTICLE INFO

Article history:
Received 4 March 2013
Received in revised form 20 May 2013
Accepted 22 May 2013
Available online 6 July 2013

Keywords:
Capacitive deionization
Hydrogen generation
$NaBH_4$
Fe–B catalyst
Carbon cloth

ABSTRACT

Sodium borohydride ($NaBH_4$) in the presence of sodium hydroxide as a stabilizer was a hydrogen generation source with high hydrogen storage efficiency and stability. The catalyst has a key role in H_2 generation reaction from $NaBH_4$. We reported that a structured Fe–B catalyst prepared by capacitive adsorption of Fe ions followed by alkaline chemical reduction step. A porous carbon clothes could hold Fe ions with capacitive current and it was reduced by $NaBH_4$ hydrolysis. The loading amount and the density of Fe–B electrodes were strongly dependent of the experiment conditions of an applied potential at the first step and the reduction time at the second step. We observed that Fe–B showed a stable hydrogen production from $NaBH_4$ without fast degradation phenomena; even if the production rate was slower than that using Co–B or Ni–B. In addition, H_2 generation rate using Fe–B/C cloth electrode can achieve 813 mL min^{-1} g^{-1} catalyst at room temperature.

1. Introduction

Along with increasing demand in using environmental friendly and efficient energy sources for transportation and domestic electronic applications, fuel cells are attracting current global attention due to their many large advantages. Among the various types of fuel cell, the proton-exchange membrane fuel cells (PEMFC) have been widely researched in recent years [1–4]. Hydrogen (H_2) can be mainly produced from chemical reactions [5], from the electrolysis of water [6], or the reforming and thermal decomposition of hydrocarbons [7]. H_2 has been stored in tanks in the form of compressed or liquefied H_2, in H_2-storing alloys, and on activated carbon or nanoscale materials [8]. However, none of these methods are suitable for portable applications due to the low volumetric and gravimetric efficiency as well as their associated safety issues. Alternative storage in forms of liquid fuels (methanol, ethanol, gasoline, etc.) and chemical hydrides ($NaBH_4$, KBH_4, LiH, NaH, etc.) could be employed as H_2 sources for portable PEMFC. In the case of the liquid fuels, high-temperature reforming processes are too complex to satisfy the requirements of portable PEMFC operation.

Among the chemical hydrides, sodium borohydride ($NaBH_4$) has been intensively studied as a H_2 storage material because of its advantages of: nonflammability and stability in air, easily controlled H_2 generation rate and side product recyclability, [8,9] and its capability of storing 10.8 wt% of H_2 [1]. The reaction product (borax) obtained after removal of H_2 from $NaBH_4$, is environmentally clean and can be recycled to generate the reactant [9]. H_2 gas can be generated by the hydrolysis of borohydride in the presence of specific catalyst at room temperature [3,10]:

$$NaBH_4 + 2H_2O \xrightarrow{\text{Catalyst}} NaBO_2 + 4H_2 \quad \Delta H = -248.9\ \text{kJ mol}^{-1}$$

The catalyst has a key role in H_2 generation reaction from $NaBH_4$. The catalysts based on noble metals such as Ru and Pt have been experimented for hydrolysis of $NaBH_4$ [11–15], but they are expensive, causing a limitation for their use. There are numerous papers reported using non-noble metal salt for the fabrication of catalyst to replace the use of noble metals. Eom et al. studied the cobalt–phosphorous (Co–P) catalysts by electroless deposition. It was found that Co–P catalysts with finer crystalline Co exhibited a higher H_2 generation rate of 3300 mL min^{-1} g^{-1}catalyst in 1 wt% NaOH and 10 wt% $NaBH_4$ solutions at 30 °C [16]. The Co and Co–P catalysts can be prepared by electroplating on Cu in sulphate-based solution with or without an addition of $H_2PO_2^-$ ions [17].

Lee studied the effect of a structured Co–B catalyst on H_2 generation from an alkaline $NaBH_4$ solution [8]. The catalyst was prepared by chemical reduction of Co precursors coated on a Ni foam

---

[*] Corresponding author at: Electrochemical Reaction and Technology Laboratory (ERTL), School of Environmental Science and Technology, Gwangju 500-712, South Korea. Tel.: +82 62 715 2440; fax: +82 62 715 2434.
E-mail address: jaeyoung@gist.ac.kr (J. Lee).

0920-5861/$ – see front matter © 2013 Elsevier B.V. All rights reserved.
http://dx.doi.org/10.1016/j.cattod.2013.05.024

support. He found that the optimum H_2 generation was obtained at a Co/B molar ratio of 1.5/2.8, with a maximum activity at temperature of 250 °C. Kim et al. [10] reported the operating conditions in a flow reactor for continuous generation of H_2: optimum flow rate of $NaBH_4$ aqueous solution at 17.5 mL min^{-1}; appropriate concentrations of $NaBH_4$ and NaOH in the feed solution at 20 and 1 wt%, respectively for the generation of H_2. The system can produce more than 6 L min^{-1} of H_2.

Fernandes et al. reported the Co/(Co + Ni) molar ratio in Co–Ni–B catalyst of 0.85 having much superior activity with the highest H_2 generation rate of 1175 mL min^{-1} g^{-1} catalyst [9]. Synergetic effect of the Co and Ni atoms in Co–Ni–B catalyst is able to lower the activation energy up to 34 kJ mol^{-1} as compared to 45 kJ mol^{-1} obtained with Co–B powder. Dong et al. studied the effect of heat treatment of nickel boride catalyst (Ni_xB) on the catalysis of $NaBH_4$ hydrolysis reaction. It was found that the Ni_xB catalyst showed great improvements in catalytic activity and operational stability after heat treatment at 150 °C in vacuum [18].

Using iron for fabrication of catalyst was studied by several reports. C. Wu et al. firstly produced ferric catalyst from reactions between pre-infused ferric salts and simultaneous feeding of $NaBH_4$ solution into a H_2 generating reactor [19]. It was found that H_2 generation route using $FeCl_3$ show excellent activity; resulting in a high H_2 generation efficiency (over 94%) and an average H_2 generation rate of 1.08 L min^{-1}. Besides, Fe also was added to Co–B catalyst by chemical reduction of the corresponding its salts [20,21]. Fe–Co–B catalyst showed significantly promoting ability of H_2 generation rate of 22 mL min^{-1} g^{-1} in a 15 wt% $NaBH_4$ and 5 wt% NaOH solutions at 30 °C, and the apparent activation energy of the hydrolysis reaction is determined to be 27 kJ mol^{-1}. The advantages of these catalyst preparation methods are cheap, simple, and better catalyst activity but difficult to control the weight of catalyst and reduction reaction rate because cannot correct chemical flow rate during reaction process.

In this study, we prepared a structure Fe–B catalyst on the carbon cloth electrodes by electrochemical adsorption techniques, capacitive deionization (CDI). CDI system is very simple and can operate continuously, thus it is easy to control the weight and structure of catalyst loading on electrodes by changing flow rate of reactants, applied voltage and time of reduction reaction. Furthermore, CDI system is versatile by used for H_2 production process with applying aqueous solution of $NaBH_4$ and NaOH following Fe–B catalyst preparation step. With this new method, the effects of the preparation conditions on the resulting catalysts' activities and H_2 production efficiency were discussed.

2. Experimental

2.1. Catalyst preparation

The carbon cloth 3 cm × 3 cm at two sides of electrodes (positive and negative) was prepared as an electrode. The structured metal-B catalysts were fabricated by chemical reaction of iron salts with borohydride solution. The $FeCl_3$ (Sigma Aldrich) and $NaBH_4$ (DAEJUNG Chemicals, South Korea) were used as a metal precursor and a reducing agent, respectively. Metal precursor solution flows into CDI system, where the voltage has been applied. Metal ions are adsorbed on positive and negative electrodes as a result of electric field created by the applied voltage. Then, CDI system is washed with dilute water in condition of applied voltage and the reducing agent, $NaBH_4$ solution, flows into CDI system for chemical reduction until iron ion is entirely converted into Fe–B catalyst (Fig. 1). The metal-B catalyst coated on carbon material by capacitive deionization was then dried at 60 °C in 6 h to remove water.

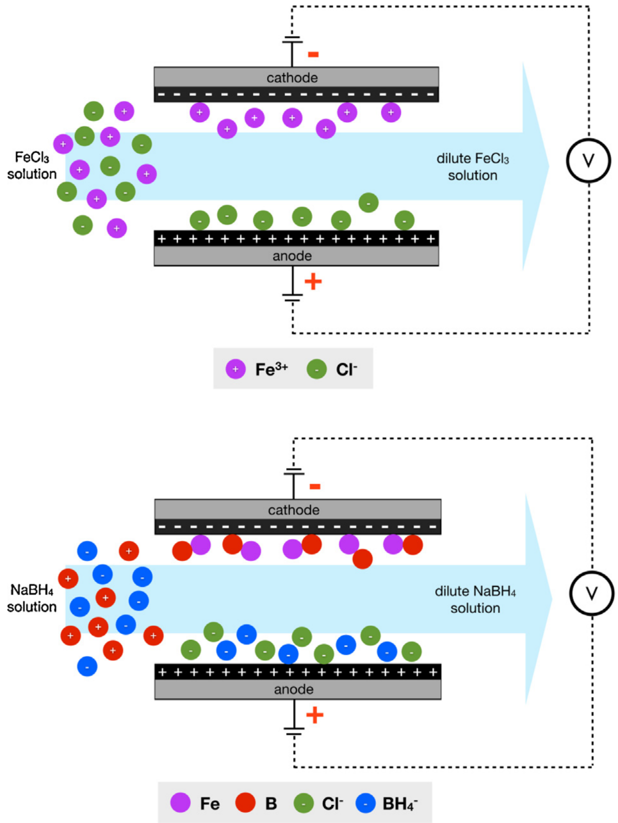

Fig. 1. Illustration of capacitive deionization process: (a) capacitive deionization process and (b) reduction reaction process.

2.2. Catalyst characterization

The morphology, physical properties, and phase structure of the prepared catalysts were characterized by several analytical methods. The surface morphology and elemental analysis of the prepared catalysts were examined by a scanning electron microscope (SEM, JEOL JSM 5200) and energy dispersive X-ray spectroscopy (EDX). The phase structures of the prepared catalyst were characterized by X-ray diffraction (XRD, Rigaku D/MAXIIIA). Surface composition and electronic state were analyzed using X-ray photoelectron spectrum (XPS, VG Multilab 2000).

2.3. Hydrogen generation test

Activities of the synthesized catalysts for H_2 production were examined in a continuous reactor which was initially used for reduction reaction of fabrication of Fe–B catalyst. The catalyst plate with the size of 9 cm^2 (3 cm × 3 cm) was loaded into the reactor and the H_2 production test was started by introducing the aqueous solution containing 20 wt% $NaBH_4$ and 1 wt% NaOH into the reactor. The temperature of solution reactor was measured by temperature meter. The products of reaction which consists of H_2 gas and water vapor is then flowed into separating instrument which contains silica gel where the water vapor is held and H_2 gas flows out and measured by the mass flow meter (Fig. 2).

3. Results and discussion

3.1. Effect of applied voltage on catalyst preparation

At this experiment, $FeCl_3$ concentration is fixed at 10 wt%, with a flow rate through the CDI system of 3 mL min^{-1} and a flow time

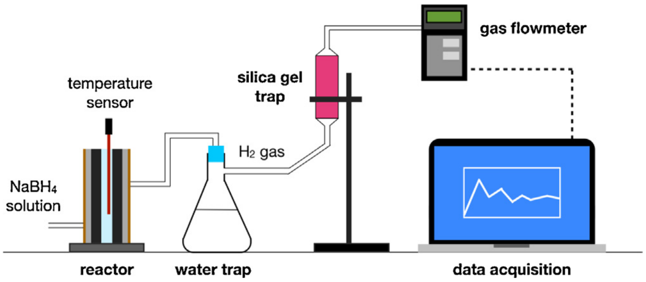

Fig. 2. Schematic diagram of H_2 generation test.

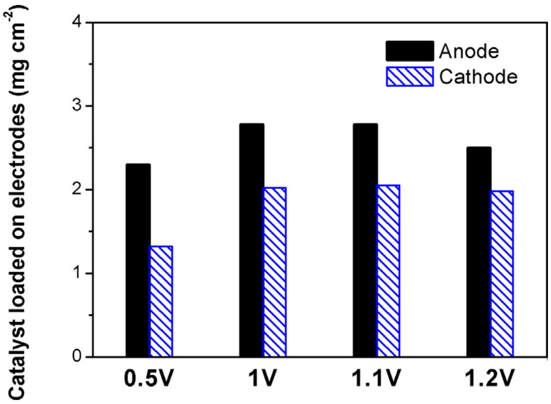

Fig. 3. Effect of applied voltage on the catalyst loading in the carbon cloth.

of 20 min. The effect was first studied by applying 0.5; 1.0; 1.1 and 1.2 V, respectively. The $NaBH_4$ and NaOH concentrations flowing into CDI system for reduction reaction are 1 and 0.1 wt%, with flow rate of 2 mL min^{-1} and the reaction time of 12 min. The coated catalyst is then dried at 60 °C for 6 h to remove humidity. The weight of catalysts is shown in Fig. 3. We found that the weight of catalysts is directly proportional to increasing of applied voltage on electrodes from 0.5 to 1.1 V and decreases slightly at 1.2 V.

Ion adsorption characteristic on electrodes also is shown in Fig. 3. Ions in feed solution are adsorbed on the surface of electrodes when a voltage is applied to the cell. It was found out that amount of catalyst at anode is larger than that at the cathode. In order to detail understand about adsorption mechanism of Fe^{3+} on electrodes (anode and cathode), we conduct reduction reaction experiment with $FeCl_2$ and $FeCl_3$ solutions and explain clearly at following parts of this study.

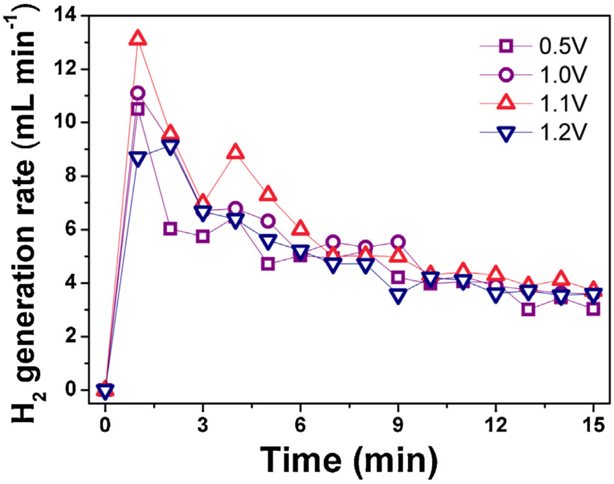

Fig. 4. Effect of applied voltage on the H_2 generation rate.

H_2 generation rate shown in Fig. 4 increases with increasing of the applied voltage from 0.5 to 1.1 V and decreasing at 1.2 V which is almost similar to the trend observed in Fig. 3. The H_2 generation rate decreases in 10 min of reaction time since the part of catalyst is detached from the electrode surface. H_2 generation rate is stable after about 10 min of the reaction process.

3.2. *Characterization of Fe–B catalyst*

Fig. 5 shows the SEM of the precipitate at the surface of carbon cloth electrodes. The precipitates are formed via the reduction reaction between Fe^{3+} ion adsorbed on electrodes and 1 wt% $NaBH_4$ reduction solution. The voltage applying in this case is 1.1 V. The catalysts with different morphology and size show various components. Catalysts found both anode and cathode also prove the adsorption ability of carbon cloth with ions and compounds during reduction reaction. Particles fully covering on the support's surface indicate good interfacial contact between the support and catalyst

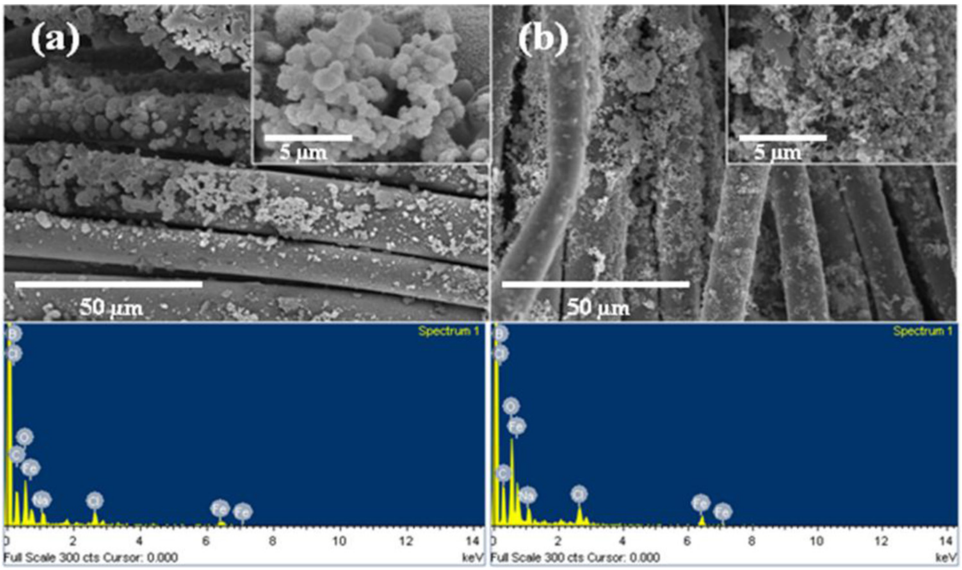

Fig. 5. SEM and EDX images of the catalyst loading on the carbon cloth: (a) anode and (b) cathode.

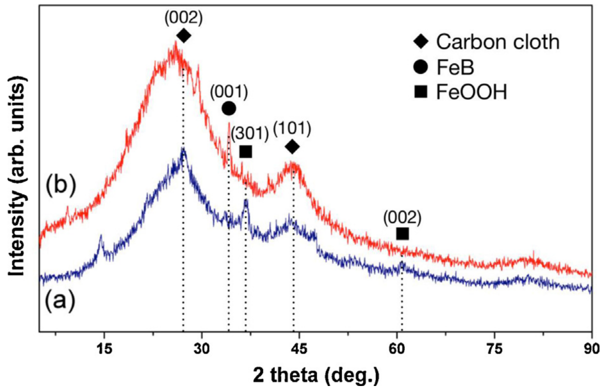

Fig. 6. XRD images of the catalyst loading on the carbon cloth: (a) anode and (b) cathode.

particle that is needed to sustain high catalytic activity, especially during the vigorous initial hydrogen generation.

EDX analysis confirmed that the principal components of the materials are boron, carbon, oxygen, and iron, as indicated in Fig. 5. The weight ratio of Fe/B at anode and cathode are 3.4:73.9 and 1.4:78.6, respectively showing easy adsorption ability of Boron on electrodes and the Fe^{3+} weight adsorbed on anode are higher than cathode.

The XRD patterns of the precipitates formed through reduction reaction process are shown in Fig. 6. The broad diffraction peaks around 23.5° (0 0 2) and 43.8° (1 0 1) are assigned to the diffraction of carbon cloth electrode [23]. The diffraction peak around 34.5° (0 0 1) is assigned to the diffraction of Fe–B, and peaks around 36.7° (3 0 1) and 61.2° (0 0 2) are assigned to the diffraction of FeOOH.

3.3. Differences between Fe^{3+} and Fe^{2+}

Adsorption of Fe^{2+} and Fe^{3+} on electrodes is investigated by reduction reaction of $FeCl_2$ and $FeCl_3$ solutions with aqueous solution of $NaBH_4$ and NaOH. Experiment condition of Fe^{2+} and Fe^{3+} is the same with 10 wt% $FeCl_3$, 10 wt% $FeCl_2$, 1 wt% $NaBH_4$ and 0.1 wt% NaOH. Applied voltage is fixed of 1.1 V. As shown in Fig. 7, amount of catalyst loaded on anode is larger than cathode with $FeCl_3$ solution and this is contrast to the case of $FeCl_2$ solution. It can be explained by processes Fe^{3+} is hydrolyzed in water and basic condition. The equations of Fe^{3+} hydrolysis reactions in water condition can be displayed as follow [22]:

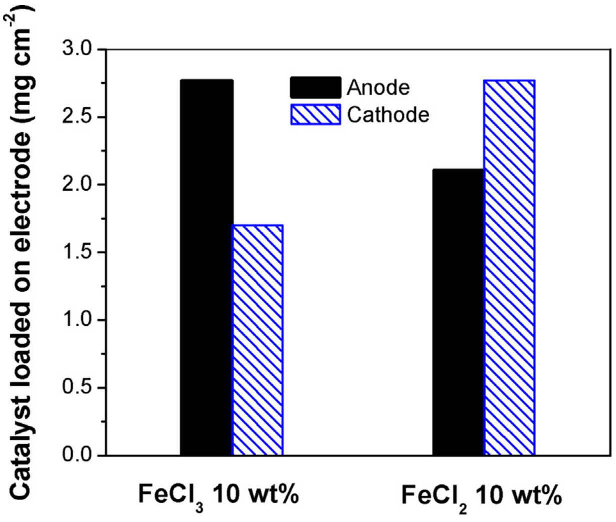

Fig. 7. Comparison of catalyst loaded on electrode using $FeCl_3$ and $FeCl_2$ solutions.

$$Fe^{3+} + H_2O \rightarrow FeOH^{2+} + H^+ \quad K1$$

$$Fe^{3+} + 2H_2O \rightarrow Fe(OH)_2^+ + 2H^+ \quad K2$$

$$Fe^{3+} + 3H_2O \rightarrow Fe(OH)_3 + 3H^+ \quad K3$$

$$Fe^{3+} + 4H_2O \rightarrow Fe(OH)_4{}^- + 4H^+ \quad K4$$

$$2Fe^{3+} + 2H_2O \rightarrow Fe_2(OH)_2{}^{4+} + 2H^+ \quad K5$$

$$3Fe^{3+} + 4H_2O \rightarrow Fe_3(OH)_4{}^{5+} + 4H^+ \quad K6$$

With K: equilibrium constant, pH = 1.24, $[Fe]_T = 0.36$ M
From $K_1 - K_6$, pH and $[Fe]_T$, we can calculate [ions]:

$$Fe^{3+} = 0.323\,M$$

$$Fe(OH)^{2+} = 3.6 \times 10^{-2}\,M$$

$$Fe(OH)_2{}^+ = 2 \times 10^{-4}\,M$$

$$Fe(OH)_3 = 2.4 \times 10^{-6}\,M$$

$$Fe(OH)_4{}^- = 7.4 \times 10^{-18}\,M$$

$$Fe_2(OH)_2{}^{4+} = 3.5 \times 10^{-2}\,M$$

$$Fe_3(OH)_4{}^{5+} = 1.5 \times 10^{-3}\,M$$

Clearly, $FeCl_3$ solution consists of main cations, very few anions, so that they will be absorbed mainly on cathode when voltage is applied. Thus, Fe^{3+} exists mainly positive charges in aqueous solution and be adsorbed on cathode during time of applied voltage. Besides, when applying solution of $NaBH_4$ and NaOH in reduction reaction of Fe–B catalyst preparation, part of these positive charges immediately combines OH^- to become negative charge $Fe(OH)_4{}^+$ and be adsorbed continuously on anode to contribute increasing catalyst loading on anode:

$$Fe^{3+} + OH^- \rightarrow Fe(OH)_4{}^- \rightarrow FeO(OH)_2{}^- \cdot H_2O$$

Negative charge phenomenon of Fe^{3+} in basic condition is not indicated with Fe^{2+} which is positive charge and to be adsorbed on cathode. Fig. 7 also shows total amount of catalyst loading on electrodes using $FeCl_2$ solution is larger than using $FeCl_3$ solution, 2.88 and 2.47 mg cm^{-2}, respectively. Clearly, adsorption ability of Fe^{2+} on electrode with applied voltage is better than Fe^{3+}. However, Fig. 8 shows that H_2 generation rate using Fe^{2+}–B catalyst is smaller than Fe^{3+}–B catalyst during experiment time. The less active ability of Fe^{2+}–B catalyst comparing to Fe^{3+}–B catalyst is explained for this result.

To determine the presence and oxidation state of iron in catalyst, we conduct X-ray photoelectron spectroscopy (XPS) measurement and the results are shown in Fig. 9. The O 1s spectra are composed of four peaks, three peaks at more 530 eV show binding state Fe_2O_3 and Fe_3O_4 and another component at approximately 531.9 eV corresponds to FeOO*H [24]. The B 1s spectra (about 192 eV) show mainly binding state of B_2O_3 and $BO_6{}^{3-}$ [24]. The elemental Fe in both catalysts (using $FeCl_2$ and $FeCl_3$ solution) with binding energies of approximately 724 and 710 eV indicated that Fe can mainly exist at Fe_2O_3, Fe_3O_4, and FeOOH states during reduction reactions of $FeCl_2$ and $FeCl_3$ solutions [24]. This also can be suggested that

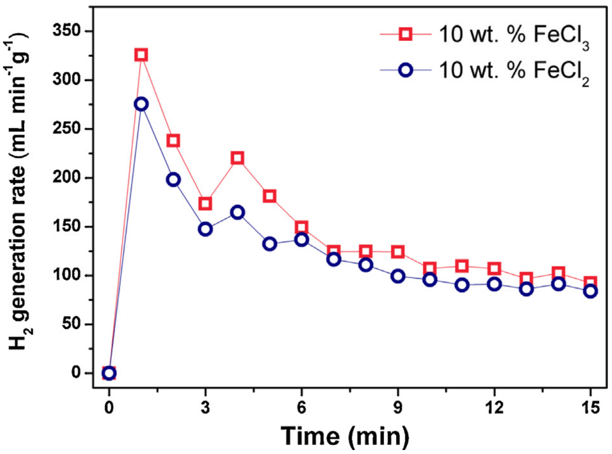

Fig. 8. H_2 generation rate using $FeCl_3$ and $FeCl_2$ solutions.

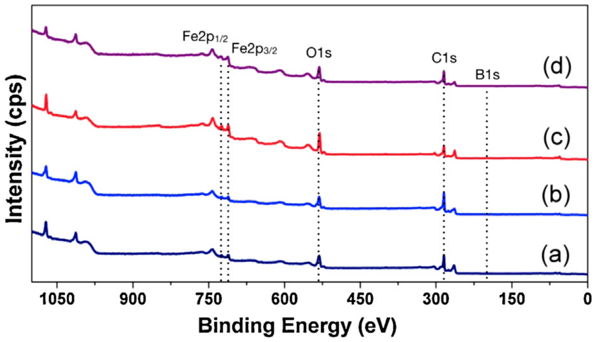

Fig. 9. X-ray photoelectron spectra of: (a) anode of Fe^{3+}–B catalyst, (b) cathode of Fe^{3+}–B catalyst, (c) anode of Fe^{2+}–B catalyst and (d) cathode of Fe^{2+}–B catalyst.

Fe^{2+} and Fe^{3+} ions (of $FeCl_2$ and $FeCl_3$ solution) change to similarly oxidized states after reduction process of catalyst fabrication.

3.4. *Effect of flow rate of $NaBH_4$ solution on H_2 generation rate*

The variation of H_2 generation rate with the flow rate of $NaBH_4$ solution is given in Fig. 10. The flow rate of the $NaBH_4$ (20 wt%) and NaOH (1 wt%) solution used was from 1 to 18 mL min^{-1} gave corresponding H_2 generate from 59 to 813 mL min^{-1} g^{-1} catalyst. These data show that a faster flow rate gives rise to increased H_2 generation. It is concluded that the H_2 generation rate is strongly dependant on the $NaBH_4$ solution flow rate at the room temperature.

The H_2 generation efficiency H is calculated via the following equation [10]:

$$H = \frac{\text{real } H_2 \text{ generation}}{\text{theorectical } H_2 \text{ generation}} = \frac{V}{u \times x/38 \times 4 \times 22.4}$$

where V is the H_2 generation rate (L min^{-1}), u the solution flow rate (mL min^{-1} ≈ g min^{-1}) and x is the $NaBH_4$ concentration. In this equation, the values 38, 4 and 22.4 represent the $NaBH_4$ molecular weight, moles of H_2 generation per a mole of $NaBH_4$ and gas volume per mole, respectively.

Fig. 10 shows the H_2 generation rate and efficiency against the flow rate. The H_2 generation efficiency increases from $NaBH_4$ flow rate of 1–2 mL min^{-1} and decrease at higher flow rates but H_2 generation rate increases linearly with increasing flow rates. Considering both H_2 generation rate and efficiency, 5 mL min^{-1} was chosen as the solution flow rate for our system.

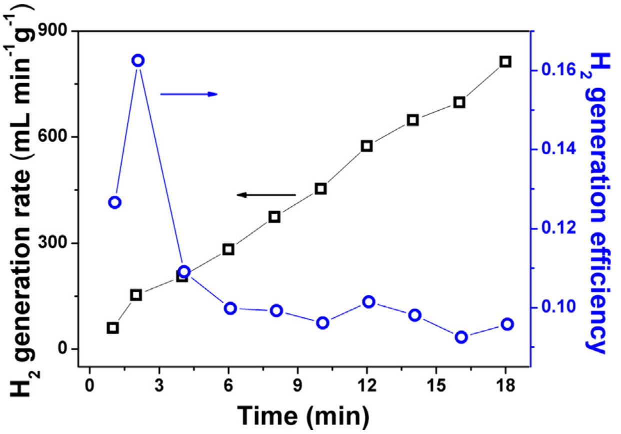

Fig. 10. Effect of flow rate of the $NaBH_4$ solution on H_2 generation rate and efficiency.

4. Conclusions

In this report, we designed experiment to study the catalyst adsorption mechanism and H_2 generation process. The voltage from power supply is determined of 1.1 V and at this voltage; the H_2 generation rate is the maximum. Adsorption of Fe^{3+} and Fe^{2+} on electrodes is entirely different. In water and slightly basic condition and applied voltage, Fe^{3+} will react with H_2O and OH^- to form negative charge $FeO(OH)_2{}^-H_2O$ and then adsorbed on anode. This is not found with Fe^{2+} since Fe^{2+} is adsorbed on cathode. The H_2 generation test also shows the less active ability of Fe^{2+}–B catalyst comparing to Fe^{3+}–B. In addition, H_2 generation rate using Fe–B/C cloth electrode can achieve 813 mL min^{-1} g^{-1} catalyst at room temperature.

Acknowledgments

This work was supported by the New & Renewable Energy Development Program of the Korea Institute of Energy Technology Evaluation and Planning (KETEP) grant funded by the Korea Government Ministry of Knowledge Economy (No. 20113020030010).

References

[1] J.C. Ingersoll, N. Mania, J.C. Thenmozhiyal, A. Muthaiah, Journal of Power Sources 173 (2007) 450–457.
[2] C. Wu, F. Wu, Y. Bai, B. Yi, H. Zhang, Materials Letters 59 (2005) 1748–1751.
[3] H. Senoh, Z. Siroma, N. Fujiwara, K. Yasuda, Journal of Power Sources 185 (2008) 1–5.
[4] B.H. Liu, Z.P. Li, Journal of Power Sources 180 (2008) 530–534.
[5] C. Wu, H.M. Zhang, B.L. Yi, Progress in Chemistry 17 (2005) 423–429.
[6] E. Rasten, G. Hagen, R. Tunold, Electrochimica Acta 48 (2003) 3945–3952.
[7] O. Yamada, Thin Solid Films 509 (2006) 207–211.
[8] J. Lee, K.Y. Kong, C.R. Jung, E. Cho, S.P. Yoon, J. Han, T.G. Lee, S.W. Nam, Catalysis Today 120 (2007) 305–310.
[9] R. Fernandes, N. Patel, A. Miotello, M. Filippi, Journal of Molecular Catalysis A: Chemical 298 (2009) 1–6.
[10] S.J. Kim, J. Lee, K.Y. Kong, C.R. Jung, I. Min, S.Y. Lee, H.J. Kim, S.W. Nam, T.H. Lim, Journal of Power Sources 170 (2007) 412–418.
[11] S.C. Amendola, S.L. Sharp-Goldman, M.S. Janjua, N.C. Spencer, M.T. Kelly, P.J. Petillo, M. Binder, International Journal of Hydrogen Energy 25 (2000) 969–975.
[12] S.C. Amendola, S.L. Sharp-Goldman, M.S. Janjua, M.T. Kelly, P.J. Petillo, M. Binder, Journal of Power Sources 85 (2000) 186–189.
[13] Z.T. Xia, S.H. Chan, Journal of Power Sources 152 (2005) 46–49.
[14] G. Guella, B. Patton, A. Miotello, The Journal of Physical Chemistry C 111 (2007) 18744–18750.
[15] R.B. Biniwale, S. Rayalu, S. Devotta, M. Ichikawa, International Journal of Hydrogen Energy 33 (2008) 360–365.
[16] K.S. Eom, K.W. Cho, H.S. Kwon, Journal of Power Sources 180 (2008) 484–490.

[17] K.W. Cho, H.S. Kwon, Catalysis Today 120 (2007) 298–304.
[18] H. Dong, H. Yang, X. Ai, C. Cha, International Journal of Hydrogen Energy 28 (2003) 1095–1100.
[19] C. Wu, Y. Bai, F. Wu, Materials Letters 62 (2008) 4242–4244.
[20] Y. Liang, P. Wang, H.-B. Dai, Journal of Alloys and Compounds 491 (2010) 359–365.
[21] N. Patel, R. Fernandes, A. Miotello, Journal of Catalysis 271 (2010) 315–324.
[22] E. Matijevíc, Journal of Colloid Interface Science 58 (1977) 374–389.
[23] J. Li, X. Wang, Q. Huang, S. Gamboa, P.J. Sebastian, Journal of Power Sources 158 (2006) 784–788.
[24] F. John, Moulder, W.F. Stickle, P.E. Sobol, K.D. Bomben, Handbook of X-ray Photoelectron Spectroscopy, Physical Electronics, Inc., Minnesota, 1995.